Perovskite Phases

Deutsche Ausgabe: DOI: 10.1002/ange.201502632
Internationale Ausgabe: DOI: 10.1002/anie.201502632

Selective Dissolution of A-Site Cations in ABO_3 Perovskites: A New Path to High-Performance Catalysts**

*Wenzhe Si, Yu Wang, Yue Peng, and Junhua Li**

Abstract: *Selective dissolution is a common corrosion process in dealloying in which an alloy is immersed in acid to remove the active element, leaving behind an inert constituent. We introduce this technique into the treatment of oxide catalysts. A three-dimensionally ordered macroporous $LaMnO_3$ perovskite has been prepared and treated with diluted HNO_3 to selectively remove La cations, acquiring a novel γ-MnO_2-like material. $LaMnO_3$ is not a satisfactory catalyst on CO oxidation. Upon the removal of La cations, the obtained sample showed a significantly higher CO oxidation catalytic activity ($T_{50}=89°C$) than the initial precursor $LaMnO_3$ ($T_{50}=237°C$) and ordinary γ-MnO_2 ($T_{50}=148°C$). A large surface area, a high degree of mesoporosity, excellent low-temperature reducibility, and especially improved surface oxygen species are deduced to be responsible for CO oxidation at lower temperatures.*

The design of high-performance catalysts by facile and universal methods has always been an important goal of research on heterogeneous catalysis.[1] A common technique in other fields, if applied in the preparation of catalysts, may have a significant effect in improving catalytic activities. Selective dissolution is such a common approach in dealloying, involving immersing an alloy in some kind of acid for a particular time to remove an active element, leaving behind an inert constituent.[2] Erlebacher and co-workers selectively dissolved Ag from Ag-Au alloys with HNO_3, resulting in the formation of a nanoporous sponge Au with a high surface area.[2a] To our best knowledge, selective dissolution has not been applied in heterogeneous catalysis until now.

Perovskites, which can be expressed with the general formula ABO_3, usually exhibit unsatisfactory performance on heterogeneous catalysis. The general explanation is that the perovskites usually possess low surface area, and the native surfaces are preferentially occupied by A-site cations, which are not catalytically active.[3] If A-site cations can be selectively removed from ABO_3, the active B-site cations will remain, and the catalytic activity of the obtained material may increase significantly.

In the ABO_3 structure, A and B cations are 12-fold coordinated and 6-fold coordinated with oxygen anions, respectively.[3a,4] A–O bonds are longer and have a higher surface energy than B–O bonds, which means that A–O bonds are easier to be attacked.[5] Herein, we investigate the possibility of selectively dissolution on A-site cations from $LaMnO_3$ (LMO) perovskites by acid treatment. A three-dimensionally ordered macroporous (3DOM) LMO material was first prepared to increase the contacting surface areas of LMO with acid. After selective dissolution, a novel manganese oxide was born with large surface area and plenty of mesoporosity. What is more, the amount and mobility of surface oxygen species were increased, which provided the novel catalyst an excellent catalytic activity on CO oxidation. Our findings suggest a new avenue for manganese oxides to improve their catalytic activities.

The treatment route for the selective dissolution is shown in Scheme 1. 3DOM-LMO was prepared by employing polymethyl methacrylate (PMMA) microspheres as the hard template according to a previously reported procedure.[6] Then the 3DOM-LMO sample was immersed in dilute HNO_3 until no obvious bubble was emerging. After selective dissolution, the sample was washed and dried. The obtained product was denoted as SD-LMO. A γ-MnO_2 catalyst was prepared by hydrothermal synthesis as a contrast. The details of sample preparation and the acid treatment process are

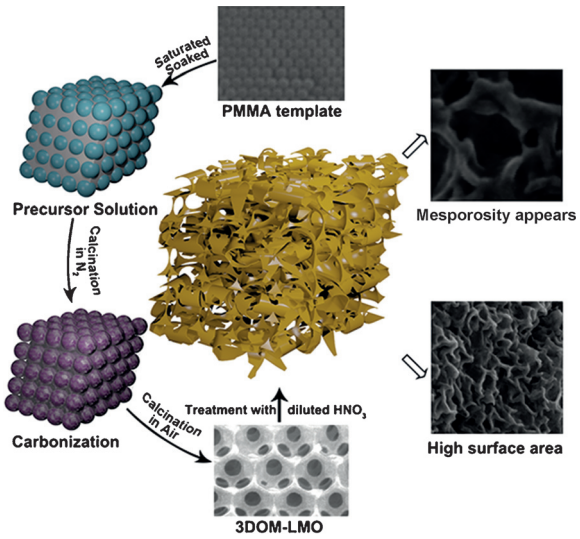

Scheme 1. Representation of the selective dissolution procedure.

[*] Dr. W. Si, Dr. Y. Wang, Dr. Y. Peng, Prof. Dr. J. Li
State Key Joint Laboratory of Environment Simulation and Pollution Control, School of Environment
Tsinghua University, Beijing 10084 (China)
E-mail: lijunhua@tsinghua.edu.cn

[**] This project is supported by the National Natural Science Foundation of China (21325731, 51478241, and 21221004) and the National High-Tech Research and Development (863) Program of China (2013AA065304).

Supporting information for this article is available on the WWW under http://dx.doi.org/10.1002/anie.201502632.

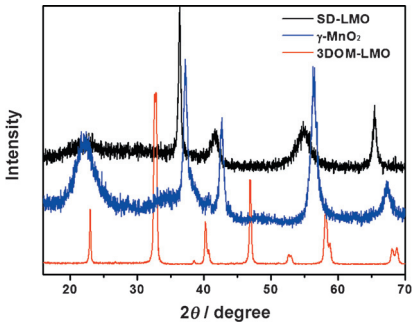

Figure 1. XRD patterns of the three samples. From bottom to top: 3DOM-LMO (JCPDS No. 50-0299), γ-MnO_2 (JCPDS No. 14-0644), and SD-LMO.

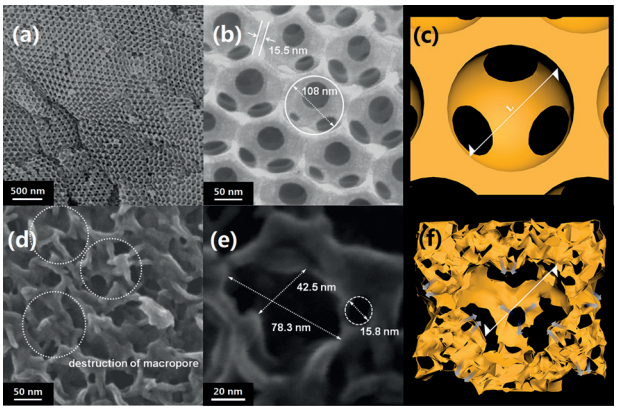

Figure 2. SEM images and representations of a)–c) 3DOM-LMO and d)–f) SD-LMO.

given in the Supporting Information. Figure 1 shows the X-ray diffraction (XRD) results of the three samples. The XRD pattern of 3DOM-LMO shows a highly crystalline character, indexed as the perovskite phase. After the acid treatment, the diffraction peaks assigned to perovskite phase disappeared, and a γ-phase MnO_2 was born. This suggests that the dilute HNO_3 can selectively dissolute La cations in LMO perovskites, leaving behind MnO_2. However, a small amount of La cations still existed with good distribution in the SD-LMO sample, according to ICP (Table 1) and TEM mapping results (Supporting Information, Figure S2). The residual La cations could attract O anions, and the Mn–O bonds would be weakened and become longer. Then the crystal size of the SD-LMO would be larger than that of the traditional γ-MnO_2. As a result, a downshift of diffraction peaks for SD-LMO can be found, compared to the γ-MnO_2 in the XRD patterns.

The morphological changes of the samples could be obviously revealed in Figure 2. The 3DOM-LMO sample exhibited a high-quality 3DOM structure. Furthermore, the macropore size and wall thickness of 3DOM-LMO were 108 ± 10 and 15.5 ± 2 nm, respectively. After the acid treatment, destruction of the 3DOM structure could be observed (Figure 2 d,e). The original smooth surface of the macropores became completely rumpled and plenty of mesoporosity appeared, which significantly increased the surface area of SD-LMO. The size of the mesoporous structure was determined to be 15.8 ± 5 nm (Figure 2 e). The results from the SEM images were consistent with those from the N_2 adsorption–desorption isotherms and pore-size distributions of these samples (Supporting Information, Figure S1). The morphological change with the acid treatment could be attributed to the shrinkage in the volume of the treated material (Figure 2 c,f). Theoretically, there is 23.9 % shrinkage in volume from $LaMnO_3$ to γ-MnO_2. Many gaps emerged as a result of the shrinkage occurring in the SD-LMO sample, which brought about many nanopores. A porous framework and high surface area are significant to improve the catalytic performance, which favor the accessibility of the reactant molecules to the catalysts.[7]

Mn $2p_{2/3}$ and O 1s XPS spectra were used to confirm the changes of electronic structure after the acid treatment, and the compositions of the surface elements are summed up in Table 1. The asymmetrical XPS peaks can be decomposed by the curve-fitting approach. As shown in Figure 3 a, the surface Mn^{4+}/Mn^{3+} molar ratio increased from 3DOM-LMO to SD-LMO after the acid treatment, which was caused by the following reaction: $2\,Mn^{3+}{}_{solid} \rightarrow Mn^{4+}{}_{solid} + Mn^{2+}{}_{liquid}$.[8] This reaction proceeded weakly in the presence of dilute HNO_3. Moreover, the Mn^{4+}/Mn^{3+} molar ratio in SD-LMO (1.02) was less than that in γ-MnO_2 (1.64), which was resulted from the remaining La cations in SD-LMO. The charge imbalance caused by additional La cations in SD-LMO can be neutralized by either Mn^{3+} or adsorbed oxygen (O_{ads}).[9] The Mn^{4+}/Mn^{3+} molar ratio was reduced and the O_{ads} was increased after the acid treatment, which could also be confirmed by O 1s XPS results (Figure 3 b).

The O_2-TPD experiments were carried out to further detect the changes of oxygen species after the acid treatment. The oxygen desorption at low temperature ($< 400\,°C$) is ascribed to O_{ads}, and the lattice oxygen (O_{latt}) starts to be released at high temperature ($> 400\,°C$).[10] From Figure 3 c, the oxygen desorption at low temperature can only be

Table 1: ICP, surface element compositions, BET surface areas, H_2 consumption, CO oxidation activity, and apparent activation energies (E_a) of the three samples.

	ICP	XPS		BET surface area	H_2 consumption	CO oxidation activity and apparent activation energy		
	La/Mn molar ratio	Mn^{4+}/Mn^{3+} molar ratio	O_{ads}/O_{latt} molar ratio	$[m^2\,g^{-1}]$	$[mmol\,g^{-1}]$	T_{10} [°C]	T_{50} [°C]	E_a $[kJ\,mol^{-1}]$
SD-LMO	0.04	1.02	0.97	245.7	9.65	34	89	26.02
3DOM-LMO	1.18	0.75	0.63	22.4	2.04	169	237	50.47
γ-MnO_2	0	1.64	0.36	68.9	10.68	92	148	38.91

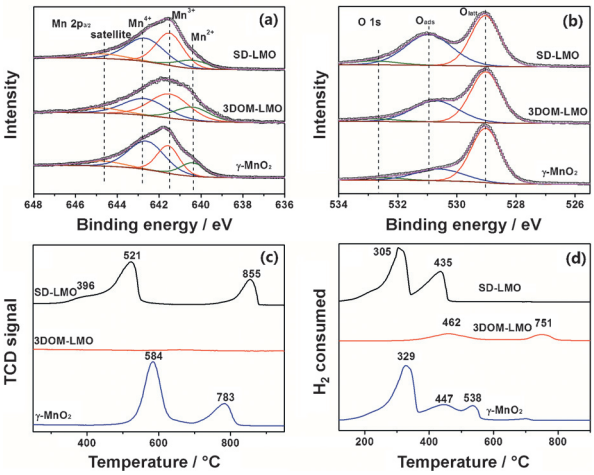

Figure 3. a) Mn $2p_{2/3}$ XPS spectra, b) O 1s XPS spectra, c) O_2-TPD profiles, and d) H_2-TPR profiles of the three samples.

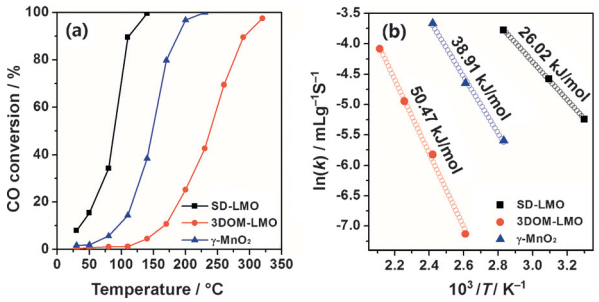

Figure 4. a) Activity profiles and b) Arrhenius plots of CO oxidation over the three samples.

observed in SD-LMO. The amount of O_{ads} in SD-LMO was much more than those in the other samples, which was consistent very well with the O 1s XPS results. Furthermore, the O_{latt} desorption temperature of SD-LMO (521 °C) was lower than that of γ-MnO_2 (584 °C). It is indicated that the O_{latt} in SD-LMO is released in a facile manner. The reason is that the Mn–O bonds in SD-LMO were weakened and got longer as a result of the residual La cations, which caused the Mn–O bonds easier to be broken.

Figure 3 d illustrates the H_2-TPR profiles of the three samples, and their quantitative analysis results are listed in Table 1. In the case of SD-LMO sample, there were two main reduction peaks at 305 and 435 °C, corresponding to a total H_2 consumption of 9.65 mmol g^{-1}. According to the results reported previously, the reduction process of manganese oxide could be reasonably divided into two sections: 1) $Mn^{4+} \rightarrow Mn^{3+}$, and 2) $Mn^{3+} \rightarrow Mn^{2+}$.[10b] The total H_2 consumption of SD-LMO was less than that of γ-MnO_2 (10.68 mmol g^{-1}). This indicated that the average valence of Mn cations in SD-LMO was lower than that in γ-MnO_2. This was also proved by Mn $2p_{2/3}$ XPS results. Besides, the reduction temperature of SD-LMO (305 °C) was lowest among the three samples, which suggested the best low-temperature reducibility and O_{latt} mobility.[11] This is in good accordance with O_2-TPD results.

The catalytic performances of the three samples on the oxidation of CO are shown in Figure 4. For the conversion of CO into CO_2, T_{10} (the temperature of the conversion 10 %) for samples 3DOM-LMO, γ-MnO_2, SD-LMO are 169, 92, and 34 °C; T_{50} (the half conversion temperature) are 237, 148, and 89 °C, respectively. The catalytic activities increased in the sequence of 3DOM-LMO < γ-MnO_2 < SD-LMO. The surface areas significantly influence the catalytic activities. The SD-LMO owned the largest surface area among the three samples. Therefore the apparent activation energy (E_a) was calculated to eliminate the effect of the surface area. The sample with lower E_a value can oxidize CO more easily.[12] From Figure 4 b, the E_a value of SD-LMO was smaller than those of the others. Based on the above analysis, CO oxidation might proceed more readily over the SD-LMO sample. The difference in E_a is most likely related to the difference in surface oxygen species. In catalytic reaction, especially CO oxidation, the Langmuir–Hinshelwood mechanism and the Mars-van Krevelen mechanism are generally proposed to be responsible for this reaction system.[13] CO is oxidized mainly by O_{ads} in the Langmuir–Hinshelwood mechanism and by O_{latt} in the Mars-van Krevelen mechanism, respectively. Thus both O_{ads} and O_{latt} play a very important role in catalytic reaction. After the acid treatment, the residual La cations not only increased the amount of O_{ads}, but also made the O_{latt} easier to be released, improving the O_{latt} mobility on the catalyst. The two mechanisms would be enhanced at the same time. Thus the SD-LMO showed the best catalytic performance. The previously reported E_a values of the various catalysts for CO oxidation are summarized in the Supporting Information, Table S1.[14] The E_a value of the SD-LMO catalyst was much lower than most of the other manganese oxide catalysts. The results from the kinetic investigations confirm that SD-LMO expressed high catalytic performance on CO oxidation at low temperatures.

In summary, we have developed a facile method to synthesize γ-MnO_2-like catalyst utilizing LMO perovskites as initial precursor. The novel catalyst exhibited large surface area, plenty of mesoporosity, and excellent low-temperature reducibility. In particular, the amount of O_{ads} and the mobility of O_{latt} were increased significantly after the acid treatment. All of these provided the novel catalyst with an outstanding catalytic activity on CO oxidation. Our findings not only suggest a new avenue for perovskite-based manganese oxides to improve their catalytic activities on heterogeneous catalysis, but also supply a method to synthesize novel γ-MnO_2-like materials, which may possess huge potential in other fields.

Keywords: CO oxidation · heterogeneous catalysis · manganites · perovskite phases · selective dissolution

How to cite: *Angew. Chem. Int. Ed.* **2015**, *54*, 7954–7957
Angew. Chem. **2015**, *127*, 8065–8068

[1] a) Z.-R. Tian, W. Tong, J.-Y. Wang, N.-G. Duan, V. V. Krishnan, S. L. Suib, *Science* **1997**, *276*, 926–930; b) J. M. Thomas, *Angew. Chem. Int. Ed.* **1999**, *38*, 3588–3628; *Angew. Chem.* **1999**, *111*, 3800–3843; c) A. T. Bell, *Science* **2003**, *299*, 1688–1691; d) S.

Bag, A. F. Gaudette, M. E. Bussell, M. G. Kanatzidis, *Nat. Chem.* **2009**, *1*, 217 – 224; e) F. Wang, C. Li, L.-D. Sun, C.-H. Xu, J. Wang, J. C. Yu, C.-H. Yan, *Angew. Chem. Int. Ed.* **2012**, *51*, 4872 – 4876; *Angew. Chem.* **2012**, *124*, 4956 – 4960; f) X. Huang, Y. Li, Y. Chen, E. Zhou, Y. Xu, H. Zhou, X. Duan, Y. Huang, *Angew. Chem. Int. Ed.* **2013**, *52*, 2520 – 2524; *Angew. Chem.* **2013**, *125*, 2580 – 2584; g) S.-H. Yu, F. Tao, J. Liu, *ChemCatChem* **2012**, *4*, 1445 – 1447.

[2] a) J. Erlebacher, M. J. Aziz, A. Karma, N. Dimitrov, K. Sieradzki, *Nature* **2001**, *410*, 450 – 453; b) S. Koh, P. Strasser, *J. Am. Chem. Soc.* **2007**, *129*, 12624 – 12625; c) R. Srivastava, P. Mani, N. Hahn, P. Strasser, *Angew. Chem. Int. Ed.* **2007**, *46*, 8988 – 8991; *Angew. Chem.* **2007**, *119*, 9146 – 9149; d) H. Zhang, M. Jin, Y. Xia, *Angew. Chem. Int. Ed.* **2012**, *51*, 7656 – 7673; *Angew. Chem.* **2012**, *124*, 7774 – 7792.

[3] a) S. Royer, D. Duprez, F. Can, X. Courtois, C. Batiot-Dupeyrat, S. Laassiri, H. Alamdari, *Chem. Rev.* **2014**, *114*, 10292 – 10368; b) J. M. D. Tascón, L. G. Tejuca, *J. Chem. Soc. Faraday Trans. 1* **1981**, *77*, 591 – 602; c) D. Neagu, G. Tsekouras, D. N. Miller, H. Menard, J. T. S. Irvine, *Nat. Chem.* **2013**, *5*, 916 – 923.

[4] J. Zhu, H. Li, L. Zhong, P. Xiao, X. Xu, X. Yang, Z. Zhao, J. Li, *ACS Catal.* **2014**, *4*, 2917 – 2940.

[5] K. Huang, X. Chu, L. Yuan, W. Feng, X. Wu, X. Wang, S. Feng, *Chem. Commun.* **2014**, *50*, 9200 – 9203.

[6] H. Arandiyan, H. Dai, J. Deng, Y. Wang, S. Xie, J. Li, *Chem. Commun.* **2013**, *49*, 10748 – 10750.

[7] a) S. Yuan, J.-L. Shui, L. Grabstanowicz, C. Chen, S. Commet, B. Reprogle, T. Xu, L. Yu, D.-J. Liu, *Angew. Chem. Int. Ed.* **2013**, *52*, 8349 – 8353; *Angew. Chem.* **2013**, *125*, 8507 – 8511; b) T. Y. Ma, S. Dai, M. Jaroniec, S. Z. Qiao, *Angew. Chem. Int. Ed.* **2014**, *53*, 7281 – 7285; *Angew. Chem.* **2014**, *126*, 7409 – 7413.

[8] S. Lee, G. Yoon, M. Jeong, M.-J. Lee, K. Kang, J. Cho, *Angew. Chem. Int. Ed.* **2015**, *54*, 1153 – 1158; *Angew. Chem.* **2015**, *127*, 1169 – 1174.

[9] C. H. Kim, G. Qi, K. Dahlberg, W. Li, *Science* **2010**, *327*, 1624 – 1627.

[10] a) Y. Liu, H. Dai, Y. Du, J. Deng, L. Zhang, Z. Zhao, C. T. Au, *J. Catal.* **2012**, *287*, 149 – 160; b) Y. Liu, H. Dai, J. Deng, Y. Du, X. Li, Z. Zhao, Y. Wang, B. Gao, H. Yang, G. Guo, *Appl. Catal. B* **2013**, *140 – 141*, 493 – 505.

[11] W. Tang, X. Wu, D. Li, Z. Wang, G. Liu, H. Liu, Y. Chen, *J. Mater. Chem. A* **2014**, *2*, 2544 – 2554.

[12] H. Arandiyan, H. Dai, J. Deng, Y. Liu, B. Bai, Y. Wang, X. Li, S. Xie, J. Li, *J. Catal.* **2013**, *307*, 327 – 339.

[13] J. Xu, Y.-Q. Deng, Y. Luo, W. Mao, X.-J. Yang, Y.-F. Han, *J. Catal.* **2013**, *300*, 225 – 234.

[14] a) S. Cimino, S. Colonna, S. De Rossi, M. Faticanti, L. Lisi, I. Pettiti, P. Porta, *J. Catal.* **2002**, *205*, 309 – 317; b) Y. Liu, H. Dai, J. Deng, L. Zhang, B. Gao, Y. Wang, X. Li, S. Xie, G. Guo, *Appl. Catal. B* **2013**, *140 – 141*, 317 – 326; c) M. Sadeghinia, M. Rezaei, E. Amini, *Korean J. Chem. Eng.* **2013**, *30*, 2012 – 2016; d) R. Xu, X. Wang, D. Wang, K. Zhou, Y. Li, *J. Catal.* **2006**, *237*, 426 – 430; e) L.-C. Wang, X.-S. Huang, Q. Liu, Y.-M. Liu, Y. Cao, H.-Y. He, K.-N. Fan, J.-H. Zhuang, *J. Catal.* **2008**, *259*, 66 – 74.

Received: March 22, 2015
Published online: May 12, 2015

